EasyChair Preprint

№ 5646

Shear Thickening Fluid Treated Space Suit Layups: Terrestrial and MISSE-9 Low-Earth Orbit Studies

Maria Katzarova, Norman Wagner, Richard Dombrowski, Miria Finckenor and Perry Gray

May 27, 2021

Shear Thickening Fluid Treated Space Suit Layups: Terrestrial and MISSE-9 Low-Earth Orbit Studies

Maria Katzarova[1], Norman J. Wagner[2]
University of Delaware, Department of Chemical and Biomolecular Engineering, Newark, DE, 19716, USA

Richard D. Dombrowski[3]
STF Technologies LLC, Newark, DE, 19713, USA

and

Miria M. Finckenor[4], Perry A. Gray[5]
NASA Marshall Space Flight Center, Huntsville, AL, USA

The durability of extra-vehicular activity (EVA) space suit layups treated with a specially formulated, low-volatility, shear thickening fluid (STF) is investigated on the exterior of the International Space Station (ISS) as part of the Materials on the International Space Station Experiment (MISSE), MISSE-9 mission. A control layup and a shear thickening fluid treated layup are exposed to the low-Earth orbit (LEO) environment for nearly one year in the Ram-orbiting direction of the ISS, where they receive exposure to atomic oxygen (AO), space radiation, large temperature variations, and a potential threat from micrometeoroid and orbital debris (MMOD) impact. In parallel to the MISSE mission, simulated space environment threats of MMOD via hypervelocity impact (HVI) testing and AO exposure studies are conducted at NASA's Marshall Space Flight Center (MSFC). The samples are examined for changes in mechanical properties and optical properties following this simulated environment exposure. MISSE-9 post-flight analyses of the samples' durability include puncture resistance and optical properties. The LEO environment effects are compared to ground controls and discussed relative to monitoring data from the MISSE experiments, including photographs, temperature data, UV intensity, and particle contamination.

Nomenclature

AO	=	atomic oxygen
EPG	=	environmental protection garment
EVA	=	extra-vehicular activity
HVI	=	hypervelocity impact
ISS	=	International Space Station
LEO	=	low-Earth orbit
m	=	mass
MISSE	=	materials on the International Space Station experiment
MMOD	=	micrometeoroid and orbital debris
MSFC	=	Marshall Space Flight Center

[1]Associate Scientist, Dept. of Chemical and Biomolecular Engineering, 150 Academy Street, Newark, DE 19716
[2]Professor, Dept. of Chemical and Biomolecular Engineering, 150 Academy Street, Newark, DE 19716
[3]Co-Founder, 18 Shea Way, Suite 101-102, Newark, DE 19713
[4]Senior Materials Engineer, Huntsville, AL 35812, Mail Code EM41
[5]Aerie Aerospace LLC, 1525 Perimeter Parkway, Suite 245, Huntsville, AL 35806

STF = shear thickening fluid
STF-LV = low-volatility shear thickening fluid
T = temperature
TMG = thermal micrometeoroid garment
v = velocity

I. Introduction

THE ILC Dover LP-developed thermal micrometeoroid garment (TMG) portion of the extra-vehicular activity (EVA) space suit worn by astronauts is tasked with protecting astronauts from potential hazards in the form of mechanical, thermal and radiation threats.[1,2] The TMG provides protection from extreme low and high temperatures, micrometeoroid and orbital debris (MMOD) particle impacts, and solar radiation present in low-Earth orbit (LEO) and beyond. For future exploration missions, the TMG also needs to shield against extraterrestrial regolith migration through to the pressure barrier portion of the space suit. Moreover, the cut-puncture resistance of the TMG is important, as sharp, cutting, and abraded features that may be present on the hand rails of spacecraft or satellites while performing physical EVA tasks may also compromise the integrity of the environmental protection garment (EPG).[3,4] The multi-layer TMG material layup must provide suitable protection without interfering with crew member mobility during EVA missions.

As NASA embarks further into space beyond LEO and to the surfaces of the Moon and Mars, the space suit worn will have to endure many environmental conditions including: (i) The presence of regolith which readily abrades suit materials and can permeate through interstices in woven fabrics used in the space suit and poses a threat to the pressure containing bladder layer. (ii) Sharp surfaces, rocks, or tools that represent potential cut or puncture hazards (iii) Exposure to radiation (iv) Temperature extremes (e.g. ~50 K in permanently shadowed regions of the Moon). Specifically, the aforementioned challenges are being considered by the designers of the proposed xEMU—Z-2 pressure garment.[5,6]

In this manuscript we describe the development of novel TMG layups containing STF-Armor™ technology that are capable of meeting the requirements of LEO for the next-generation of space suits. This is ongoing work under a NASA STTR Phase II award. STF-Armor™ uses shear thickening fluids (STFs), which are colloidal suspensions of nano-sized particles in a carrier fluid. STFs exhibit a novel rate-dependent mechanical response such that high stresses can nearly instantaneously transform the material from a liquid-like state into a solid-like state, imparting significant impact resistance.[7,8] While the impact mitigating properties of these fluids are significant, high-strength textiles intercalated with an STF fluid result in nanocomposite materials known as STF-Armor™, which offers advanced protection against a variety of mechanical threats.[9,10] We recently documented advances in addressing these key technological challenges through the use of novel, shear-thickening intercalated textiles (STF-Armor™) with "lotus leaf" coatings that prevented dust infiltration and greatly improved puncture resistance of the EPG.[11]

Furthermore, it is possible to experimentally simulate aspects of the LEO environment on Earth including AO exposure, UV radiation, MMOD impacts via hypervelocity impact (HVI) tests, and micro gravity. In parallel with the MISSE-9 mission, we partnered with NASA's Marshall Space Flight Center to simulate the effect of AO and HVI resilience of the MISSE-9 samples. The optical properties, which directly influence the thermal properties of a material, were also measured pre- and post-AO exposure. Moreover, post MISSE-9 flight analyses including puncture and optical properties were also performed. The MISSE exposure experiments together with the LEO environment simulation studies will help raise the TRL (technology readiness level) of this new puncture-resistant EPG technology. Moreover, the results were leveraged to coating-based solutions on samples tested on MISSE-10 (complete) and MISSE-13 (in orbit).

The paper is organized as follows: After an overview of the samples flown and their duplicates used as ground controls and for LEO environment simulation studies, the methods and results are provided concerning the ground-based studies performed at Marshall Space Flight Center with an emphasis on the effects to MMOD and optical properties. Following this, the monitoring data from the MISSE-9 flight are presented and analyzed. Finally, the post-flight results obtained from the MISSE-9 samples of these novel EPG layups are presented and discussed.

II. Background

A. Thermal Micrometeoroid Garment (TMG)

The standard TMG layup used on the International Space Station (ISS) is comprised of, beginning with the outermost layer: (i) Orthofabric, a composite woven textile of Gore-Tex® / Nomex® / Kevlar® and is the sacrificial layer of the space suit against potential hazards including but not limited to impacts of MMOD and contact with

sharp surfaces. This top layer is followed by several layers of aluminized Mylar® for protection against radiation as well as thermal temperature control. The number of layers of the aluminized Mylar® also provide a standoff distance, thereby helping to further dissipate the energy of projectile (MMOD) impact. Next, the TMG liner, here referred to as the absorber layer, helps to prevent puncture of the pressure containment layer referred to as the bladder layer. The absorber layer is neoprene-coated ripstop nylon and the bladder is polyurethane-coated nylon. Note that an additional Dacron restraint layer between the absorber layer and bladder layer will not be included in the layup studies presented in this work as it is located behind the absorber layers which are of primary interest in this work and are amenable to shear-thickening fluid intercalation.

B. STF-Armor

Previous studies,[12] where the neoprene-coated nylon absorber layer in a baseline TMG was replaced with STF-treated Kevlar® (STF-Armor) demonstrated a meaningful improvement in the quasi-static puncture resistance of the TMG space suit layup in a mass-efficient manner with flexible and lightweight nanocomposites. Furthermore, in that work, hypervelocity impact (HVI) tests revealed that an STF-Armor layup performed nominally similar to the baseline layup, preventing puncture of the life-essential bladder layer with a high-speed projectile (0.4mm, 4.84 km/s). In the work presented here, we test the performance of a LEO-compatible STF formulation using a low-volatility suspending fluid (STF-LV) capable of meeting the high-vacuum requirement of LEO. The Orthofabric top layer is also replaced with an STF-LV-treated Orthofabric layer and the neoprene-coated nylon absorber layer is replaced with two layers of STF-LV-treated Spectra®, a high- molecular-weight polyethylene woven fabric. This STF-LV-treated TMG layup and a control one with non-treated layers are tested on the Materials International Space Station Experiments, MISSE-9 mission. Note, the STF-LV-treated layup retains nominally similar weight and thickness attributes as the aforementioned STF-Armor layup.

C. Materials on the International Space Station Experiment (MISSE)

The MISSE testing platform is an external ISS facility for materials testing. Originally conducted by NASA, the research is now facilitated by Alpha Space Test and Research Alliance with MISSE-9 being its flagship mission. The MISSE-Flight Facility provides materials durability testing in the harsh environment of LEO including thermal cycling, AO exposure, cosmic radiation and potential MMOD impacts. The degree of severity of any one of these effects depends on the ISS-orbiting direction and the platform accommodates Ram, Nadir, Wake, and Zenith exposure. Alpha Space provides researchers monthly photographs of their samples as well as monitoring services including temperature measurements, UV intensity, and particle contamination which will be presented in this work.

III. Sample Materials and Methods

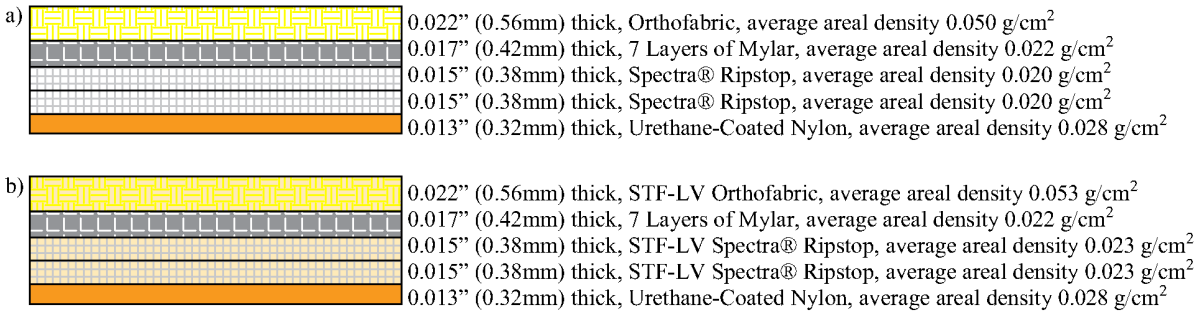

Figure 1. MISSE-9 layups: a) non-treated and b) STF-LV-treated.

There are two types of layups, a non-treated or "neat" and an STF-LV-treated layup. Cross sections of the layups are shown in Figure 1 a) and b), respectively. The neat layup will consist of Orthofabric (outermost) followed by seven layers of aluminized Mylar® and two absorber layers of Spectra®. The innermost layer will be urethane-coated nylon or the "bladder" layer. The bladder layer in these studies serves as a witness layer to any through damage that may occur during the mission or HVI testing. The STF-LV-treated layup sample will consist of STF-LV Orthofabric followed by seven layers of aluminized Mylar® and two absorber layers of STF-LV-treated Spectra®. Here too, the innermost layer will be urethane-coated nylon. Nominal thickness and areal density for each of the layers are shown.

The STF-LV formulation is a high loading (72% by weight) of nano-sized silica particles suspended in a low-volatility hydrocarbon oil. An appropriately dosed dispersant was used to distribute the polar silica particles in the hydrophobic carrier fluid homogeneously. The suspension is diluted with 1-Pentanol and used as an immersion bath. A probe sonicator was used to mix the diluted fluid. The materials are immersed for one minute in the bath and subsequently passed through nip rollers after which they are dried in an oven to evaporate off the 1-Pentanol and leave the STF-LV intercalated into the material.

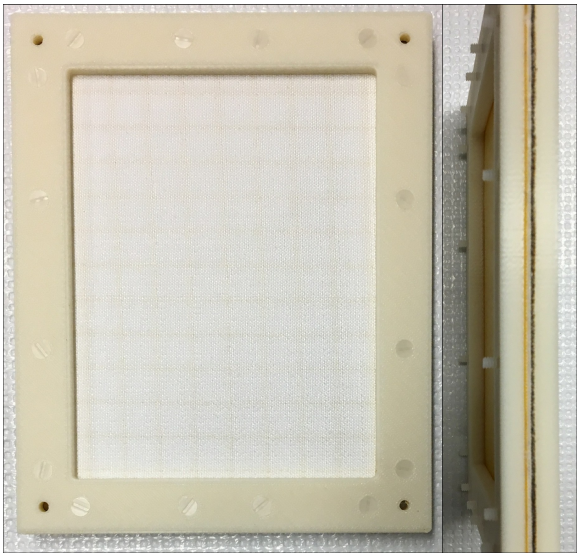

Figure 2. Top and side views of an ABS polymer mock-up of the MISSE-9 frame assembly with neat layup.

In total, four sets, where a set is a neat and a treated layup, were produced. Two sets were reserved for the MISSE-9 mission and the remaining two sets were used for simulation studies on Earth. From the two MISSE-9 sets, one was flown on the ISS while the other remained on Earth as a control against which to compare the change in performance post flight. Of the two sets which remained on Earth, one was exposed to AO and subsequently HVI tested while the other set was only HVI tested in order to infer performance changes due to AO exposure. An image of the neat layup inside a 3D-printed acrylonitrile butadiene styrene (ABS) polymer frame used for the simulation studies is shown in Figure 2. The frame is a mock-up of the MISSE-9 frame, which is constructed out of anodized aluminum. The outer dimensions of the frames are 5.65 × 7 inches with a 0.75 inch border leaving an exposed experiment area of 4.15 × 5.5 inches. The frame plates are 0.25 inch thick. The dimensions of the samples will match those of the outer dimensions of the frames (5.65 × 7 inches). The lower frame is threaded for 16 6-32 screws. The presence of AO in the LEO environment can be destructive to polymeric materials and it will be necessary to understand the effect of AO on the STF-LV formulation. In addition, albeit of low probability, impacts of MMOD in LEO are possible and understanding the STF-LV-treated materials' performance is vital. Simulation studies of these LEO challenges of AO exposure and HVI testing were performed at NASA's Marshall Space Flight Center.

Two layups, a neat and STF-LV-treated, underwent LEO environment exposure as part of the Materials International Space Station Experiments, MISSE-9 mission, deployed on the ISS and launched April 2, 2018 by SpaceX cargo-resupply mission CRS-14. The layups were tested for durability in LEO against thermal cycling, AO exposure, cosmic radiation and potential MMOD impacts. The layups were located on the exterior of the space station and oriented in the Ram-orbiting direction of the ISS (Fig. 3). The experiment duration was for one year. During this time high-definition photos and monitoring data including temperature, UV intensity, and particle contamination were relayed to us monthly. Upon return to Earth, the exposed samples were evaluated visually, gravimetrically and their durability determined by mechanical and optical properties measurements. The duplicate set of layups, which remained on Earth as ground controls to the layups in LEO were used to establish relative differences in performance and appearance of the samples flown in LEO.

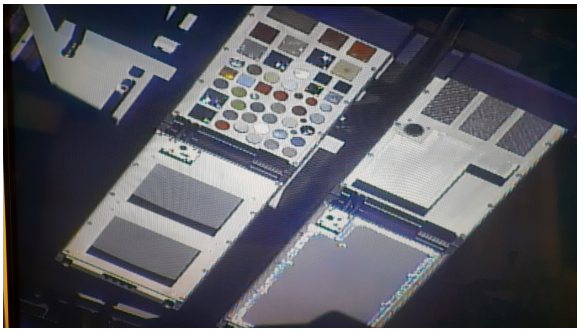

Figure 3. University of Delaware MISSE-9 experiment (two rectangular samples, bottom left corner) during LEO exposure deployed on the MISSE-FF. Image: Alpha Space Test and Research Alliance.

IV. LEO Environment Simulation Studies

A. Atomic oxygen exposure and optical properties

The presence of atomic oxygen in low-Earth orbit can lead to reactivity with exposed material surface areas. In particular, AO reacts with polymeric materials leading to erosion of the sample.[13] It is possible to simulate the effect of atomic oxygen exposure on our samples here on Earth. Atomic oxygen exposure experiments were performed at NASA's Marshall Space Flight Center. Both the neat layup and the STF-LV-treated layup were exposed to 1.7×10^{20} atoms/cm^2. The AO exposure is commensurate with the maximum allowed for a space suit or 50 EVAs × 6 hours/EVA, assuming the entire time was spent in the Ram direction.

Solar absorptance and infrared emittance were measured for the neat and STF-LV-treated layup pre- and post-AO exposure. The results are shown in Table 1. The % reflectance was also measured pre- and post- AO exposure and the results are shown in Figure 4. Overall, the reflectance of the STF-LV layups is lower than that of the neat layups in the low-wavelength regime and the high-wavelength regime both pre- and post-AO exposure. Moreover, AO exposure leads to further reduction on the low-wavelength reflectance of STF-LV-treated layups. We hypothesize that this observation may suggest that STF-LV layups could be susceptible to some solar radiation (low-wavelength) damage in the LEO environment. However, as shown in Table 1, the overall changes in infrared emittance between neat and STF-LV treated samples, as well as pre- and post-AO exposure are minimal or within uncertainty for both absorptance and emittance, with the largest effect being the ~20% increase in solar absorptance upon STF-LV treatment. Such an increase in solar absorptance may adversely affect the heat rejecting properties of the layup and warrants future quantification of the effect and investigation of coatings capable of achieving the desired optical characteristic.

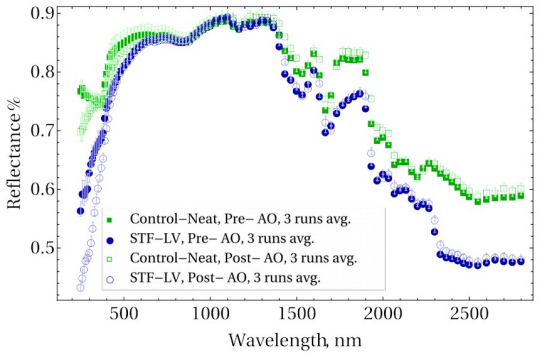

Figure 4. Reflectance measurements for a neat and STF-LV-treated layup pre- and post-AO exposure performed at MSFC.

Table 1. Optical properties of neat and STF-LV-treated space suit layups pre- and post-AO exposure.

	Solar absorptance	
Sample layup	Pre-exposure	Post-exposure
Neat	0.167 ± 0.010	0.169 ± 0.013
STF-LV	0.197 ± 0.004	0.207 ± 0.006
	Infrared emittance	
Neat	0.863 ± 0.006	0.877 ± 0.006
STF-LV	0.897 ± 0.006	0.893 ± 0.006

B. Hypervelocity Impact (HVI) Testing

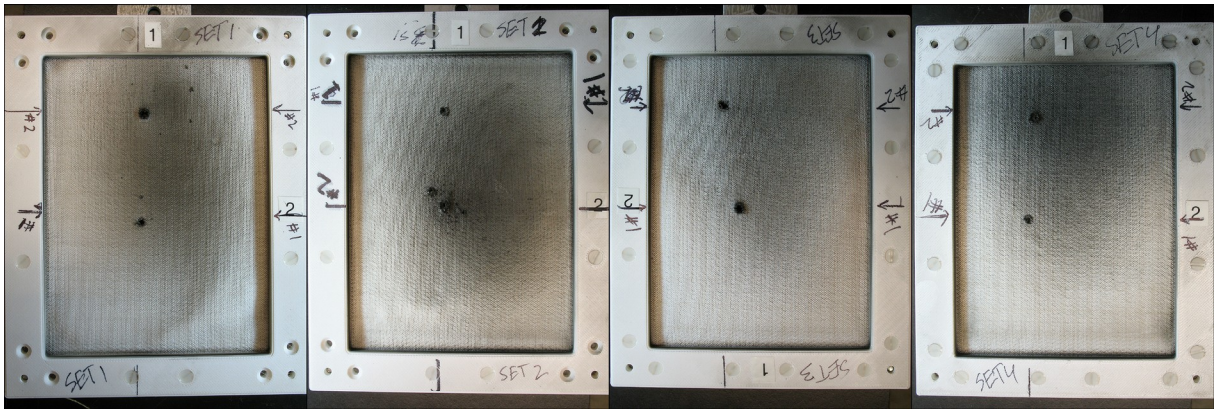

Figure 5. Frame assemblies post-HVI testing. From left to right: Set 1 (non-treated, AO exposed), Set 2 (STF-LV-treated, AO exposed), Set 3 (non-treated, non-AO exposed), Set 4 (STF-LV-treated, non-AO exposed).

Hypervelocity impact studies were performed at MSFC's Impact Testing Facility.[14] The tested layups are two neat and two STF-LV-treated for a total of four layups. As mentioned previously, all four layups will be HVI tested however a set of a neat and an STF-LV layup will also be exposed to AO prior to HVI testing to determine if AO exposure affects the ballistic performance of the layups. The configuration of the samples for the HVI tests held together in 3D-printed ABS frames is shown in Figure 2. A witness plate was mounted behind each layup to capture damage from any fully penetrating particles. Four layups in total were shot twice/layup with 2mm nominally-sized high precision nylon spheres, once at a speed of 2 km/s and a second time at a speed of 4 km/s. All impacts were 0° normal to the surface and at ambient conditions. The weight of the spheres is nominally 4.56 ± 0.03 mg. Images of the four layups post-HVI testing are shown in Figure 5. A summary of the shot velocities and calculated kinetic energies at impact, ½ mv^2, is shown in Table 2. Note that comparisons between these HVI results and those for previously studied STF-Armor-based TMG layups[12] were not possible due to the difference in pellet material type and achievable shot kinetic energies.

Table 2. HVI testing of STF-LV space suit layups. Pellet velocities and kinetic energies at impact.

	Shot	v [km/s]	½ mv^2 [J]
Neat Layup Set 1 (AO+HVI)	1	2.1772	10.80
	2	4.1203	38.66
STF-LV Layup Set 2 (AO+HVI)	1	2.1955	10.98
	2	4.0362	37.10
Neat Layup Set 3 (HVI only)	1	4.096	38.21
	2	2.4076	13.20
STF-LV Layup Set 4 (HVI only)	1	2.0358	9.44
	2	3.9749	35.98

The 2 km/s shots are at the low end of the capabilities of the gun at the MSFC facility. Unfortunately, at these kinetic energies the bladder layer was fully penetrated (perforated). Nevertheless, microscope images of each perforation on the reverse side of the top sacrificial layer, both absorber layers and the bladder layer are shown in Figure 6. The images are taken at the same magnification allowing for relative comparisons between images. First we consider the 2 km/s shots which were exposed to atomic oxygen and compare the non-treated layup (Set 1) with the STF-LV-treated layup (Set 2). The damage to the back of the STF-treated layers (Orthofabric, Spectra® 1 and 2) appears smaller than that for the corresponding non-treated layers. The damage to the bladder layer is nominally the same in both cases. The perforation of the bladder suggests that projectile integrity was not sufficiently diminished by engaging with the Orthofabric layer. The same relative comparison can be made for Sets 3 and 4 which were not exposed to atomic oxygen. The damage to the STF-treated layers (Set 4) is nominally smaller compared to the non-treated layers (Set 3). Furthermore, the layups not exposed to atomic oxygen show more burn damage around the

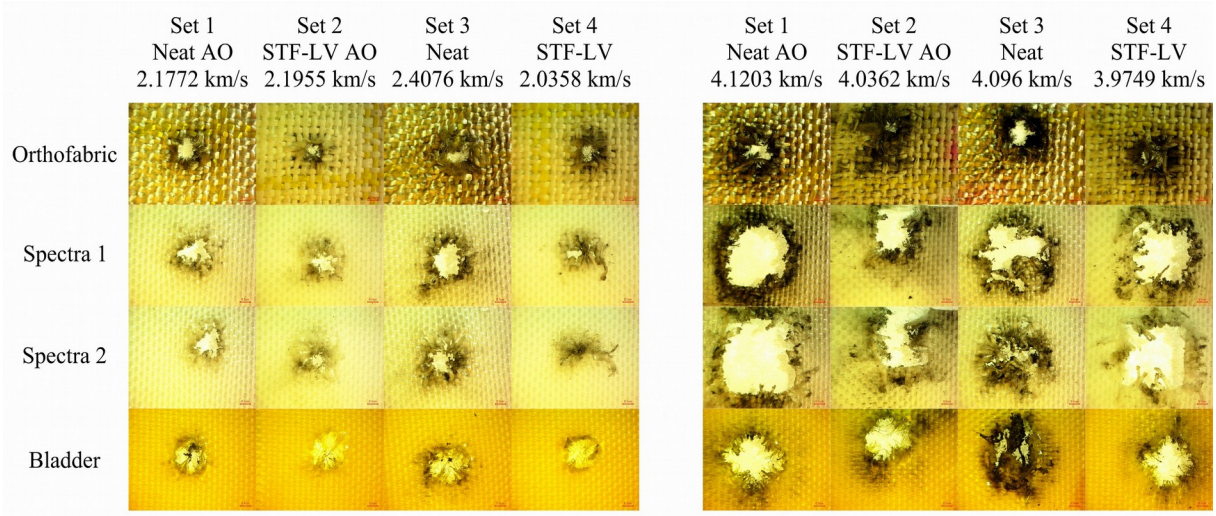

Figure 6. Back view of the sacrificial, absorber layers 1 and 2, and the bladder layer post-HVI testing. 2 km/s nominally shot layers (left) and 4 km/s (right). Scale bar length is 1 mm.

perforation perimeter. The 4 km/s projectiles are much more energetic and consequently cause significantly greater damage as can be seen in Figure 6. Overall, the results of these limited HVI tests do not show a clear pattern of improvement for the overall layups with STF-LV treatment albeit the individual such layers appear less damaged. The bladder penetration is nominally similar for all tests. In Figure 7, the eight shots are plotted against the bladder ballistic limit curve of a basic layup.[15] Additionally, the bladder perforation threshold, 3.2 J of kinetic energy, is also shown. It can be observed that all eight shots are above the predicted ballistic limit. Also, the calculated kinetic energies of the projectiles are roughly three and ten times larger than the ballistic limit for bladder integrity, for the 2 km/s and 4 km/s shots respectively. This confirms that the HVI tests should show full penetration, as observed.

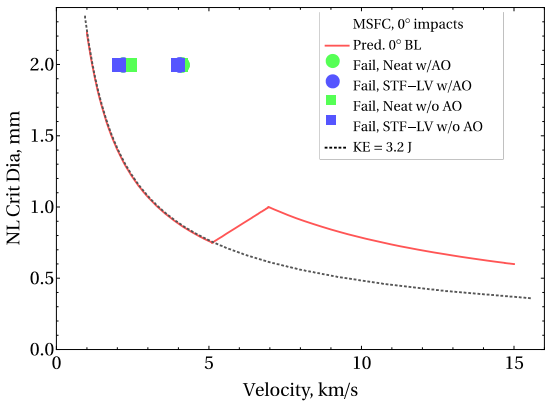

Figure 7. Comparison of the nylon projectile-based ballistic limit prediction (red line) with the shots (symbols) performed in this study. 0° impact angle.

C. Quasi-static Hypodermic Needle Puncture

Tests to simulate the potential cutting threat from sharp edges and objects were performed as quasi-static puncture tests using methods reported previously.[11] The tip of a hypodermic needle has both cutting and puncture features. In this test an ASTM F-2878 cut-puncture 21-gauge hypodermic needle is driven through normal to the surface of the sample at a rate of 10 mm/min. The test was performed for sections of Sets 1-4 of the work here as well as a control neat and a control STF-LV layup that have not been exposed to AO or HVI testing. Puncture results of the layups are shown in a box plot in Figure 8. The small square in each box is the mean puncture force based on eight punctures, the height of the box represents one standard deviation above and below the mean, the whiskers indicate the maximum and minimum recorded puncture force, and the horizontal line in the middle of the box is the median. A summary of the puncture forces, areal density and energy absorbed for each puncture are tabulated in Table 3. Overall, for each of the three comparisons, the STF-LV layup performs better than the neat layup. Furthermore, AO exposure did not degrade the quasi-static puncture test performance of the STF-LV treated layups.

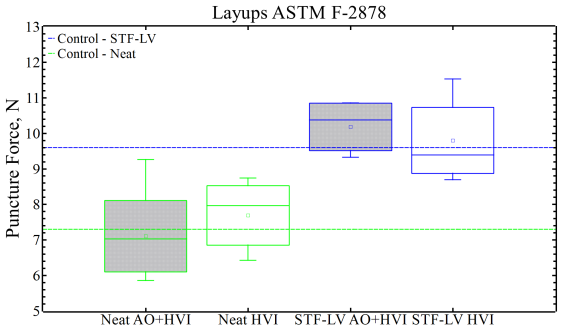

Figure 8. ASTM F-2878--Hypodermic needle puncture--maximum puncture force statistic representation after AO exposure and HVI testing.

Table 3. ASTM F-2878 puncture results of Earth-based studies.

	HVI+AO Neat (Set 1)	HVI Neat (Set 3)	HVI+AO STF-LV (Set 2)	HVI STF-LV (Set 4)
Areal Density, g/m^2	1389	1352	1525	1513
Puncture force, N	7.1+/-1.0	7.7+/-0.8	10.2+/-0.7	9.8+/-0.9

V. Flight Monitoring

The facilitators of the MISSE experiments, Alpha Space Test and Research Alliance, provided monitoring data including monthly photographs and sensor data. The sensor data includes temperature *T*, UV intensity, and particle contamination. Particle contamination data is collected by a Temperature Controlled Quartz Crystal Microbalance (TQCM) instrument. In Figure 9 are shown the very first and last set of images taken of the samples during the MISSE-9 mission. A camera trolley travels from the top to the bottom of the samples' deck taking photographs. The size of the samples is large enough requiring several images over the samples. Hence, the image shown is a stitch of 24 photographs. The shown photographs have been defished. Note, visible vertical bars are part of camera truss and not the samples. Temperature sensor data are measurements taken of the underside temperature of the samples' deck. Sensor measurements for all three sensors are recorded at the same time for a portion of time. An example of one period of measurements is shown in Figure 10. This is the first data recording period from the MISSE-9 mission. All of the data received for each of the months of flight can be provided upon request. In Figure 10, we observe a periodicity commensurate with the ISS Earth orbit time, ~90 minutes. In addition, an increase in temperature is in sync with an increase in UV intensity and corresponds to an increase in particle deposition on the microbalance. From the entire set of data points recorded of the temperature, the maximum and minimum temperatures are shown in Figure 11. The maximum temperature recorded twice was 150.2 °F (65.7 °C) on July 14, 2018 and July 26, 2018 and the minimum temperature recorded was 8.5 °F (-13.1 °C) on Dec 20, 2018. During the MISSE-9 mission, several temperature anomalies were recorded, high (eight measurements at 999.9 °F) and low (-431.9 °F and -403.7 °F) ones.

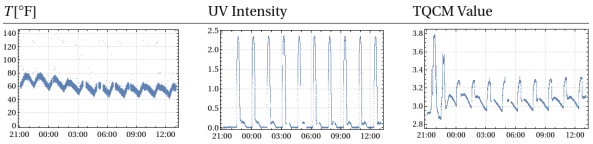

Figure 10. Sensor measurements in increments with start time Thursday April 19, 2018 21:04:41 and end time Friday April 20, 2018 13:04:15.

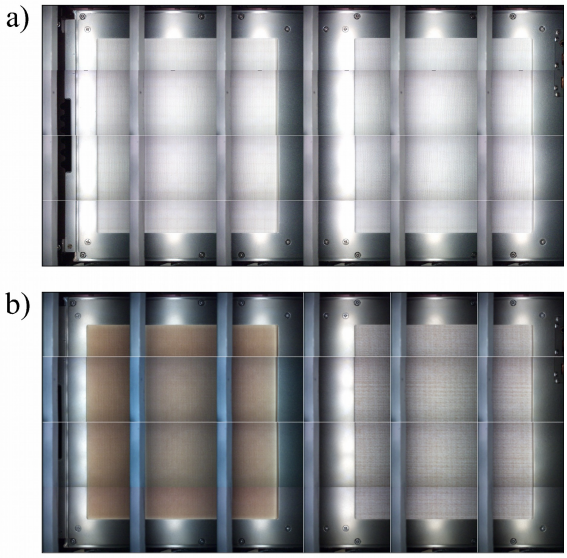

Figure 9. In vivo LEO photographs of the MISSE-9 STF-LV layup (left-oriented) and neat layup (right-oriented). a) April 23, 2018, b) October 1, 2019. Images: Alpha Space Test & Research Alliance.

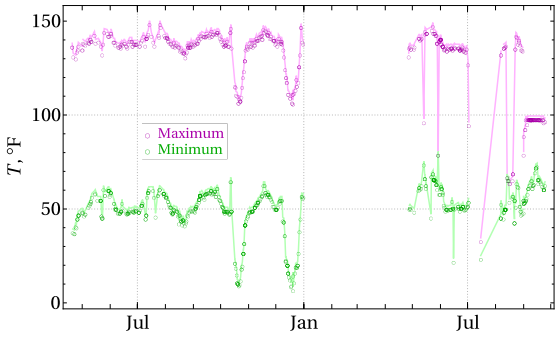

Figure 11. Temperatures recorded in °F beginning April 19, 2018 through September 24, 2019. Maximum (open magenta circles) and minimum temperatures (open green circles) measured throughout the duration of the MISSE-9 mission. Lines are only guides to illustrate the sequence of the measurements.

VI. Post-flight Testing

Post-flight tests and analyses were performed including puncture, scanning electron microscopy (SEM) imaging, photography of the layers, and optical properties measurements. The latter were again performed by our partners at MSFC. The top-facing image in Figure 12 was taken post-flight. This image shows the layups in their respective frames with the STF-LV on the left and the neat layup on the right. It can be clearly observed that the treated Orthofabric is more discolored relative to the neat Orthofabric. The significant difference in optical properties is quantified in Figure 14 where a comparison is made between the ground controls and the flown samples' reflectance proprieties. Furthermore, the measured post-flight solar absorptivity of the STF-LV-treated Orthofabric layer is 62 % higher compared to the non-treated Orthofabric post flight. Note that HVI testing of the flown samples could not be arranged after the samples' return from orbit and will warrant future studies.

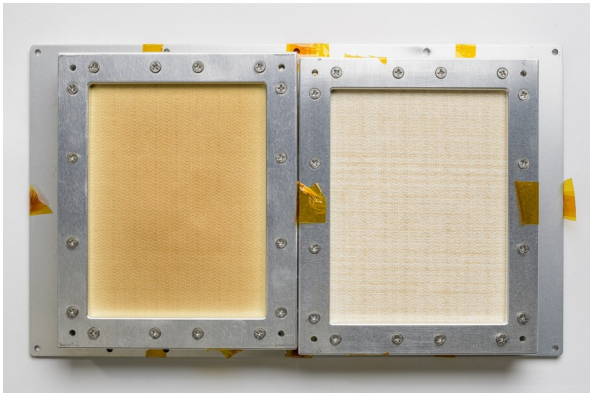

Figure 12. Post-flight MISSE-9 mission samples photograph. STF-LV-treated layup left, neat layup right. Image: University of Delaware.

Puncture tests using an ASTM F-1342 puncture probe were also performed with the layups and the individual layers. Individual layer punctures of the non-treated and STF-LV-treated Orthofabric, Spectra® absorber 1 and Spectra® absorber 2 were performed. The box plots in Figure 13 summarize the test results for Orthofabric. On average, the ISS-exposed Orthofabric performed 15% better relative to the terrestrial control. Note, the performance of the absorber layers is nominally the same and is not shown here. In order to further probe the reason for the difference in performance for the Orthofabric, stereoscope images of the outer face of the layer revealed a type of residue. Moreover, the same residue did not appear on the reverse side of the layer.

The SEM images shown in Figure 15, represent a progressive zoom of a portion of the samples flown on MISSE-9, ground controls, and those from the MSFC simulation studies for both the non-treated and STF-LV-treated Orthofabric. Specifically, we are imaging the outer-facing side of the Orthofabric, or the Gore-Tex® face. It can be observed that there is a notable difference in appearance between the terrestrial control and MISSE-9-flown material for both the neat and treated samples. In particular, the flown STF-LV samples reveal a type of topography that is not present in the terrestrial controls samples. Given the Ram-facing orientation of the samples, and hence exposure to both AO and solar radiation, a comparison with the MSFC AO-exposed samples was made in order to decouple the effect of AO or radiation on the flown samples. The MSFC samples did not undergo UV-exposure testing. It can be observed in Figure 15 that to a lesser degree, the bumpy features observed on the flown samples are also present in the AO-exposed samples suggesting AO reacts with the STF-LV formulation. The STF-LV-treated Orthofabric top surface is a composite system of the STF-LV formulation and the Gore-Tex® face. Moreover, the STF-LV formulation is comprised primarily of nano-sized silica (SiO_2) particles suspended in a hydrocarbon low-volatility fluid. Previous studies indicate erosion effects by AO are greatly reduced for silicone-based materials.[16]

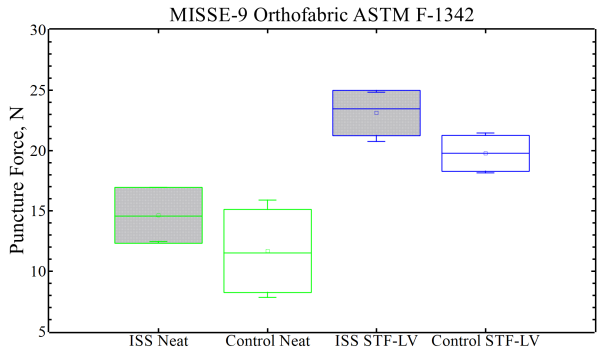

Figure 13. Orthofabric ASTM F-1342 puncture comparison of flown MISSE-9 samples and ground control samples.

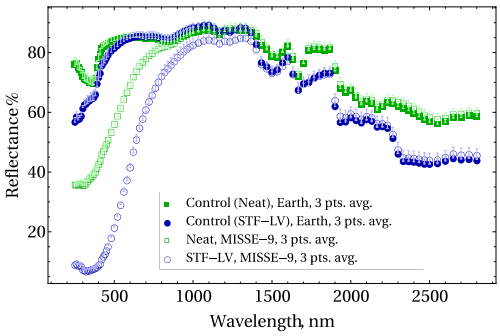

Figure 14. Reflectance measurements comparison post-LEO exposure for a neat layup and an STF-LV layup, between ground controls and MISSE-9-flown samples.

In fact, it was shown the near surface loses its organic components and forms an SiO_2 protection layer. In our STF-LV formulation, the presence of SiO_2 particles forms such a protective layer inherently. Furthermore, AO attack in the presence of UV radiation as is the MISSE-9 LEO environment, cross-links volatiles formed by the AO attack on the C-H suspending fluid used in our formulation. In summary, it may be inferred that the synergy between the mass reducing effect of AO is balanced by the cross-linking caused by UV in the presence of silica particles helping to explain the increase in puncture force. Furthermore, Teflon™ (Gore-Tex®) is very susceptible to erosion by AO. The 10^4 times magnified SEM image of the non-treated MISSE-9 Orthofabric reveals surface features consistent with erosion. The effect is observed to a lesser extent in the simulated AO exposure tests at MSFC granted the simulated exposure time was significantly lower than that during the MISSE-9 experiment. Moreover, those tests were not compounded by the additional exposure to radiation as they would experience in LEO. The results presented here appear consistent with those findings. The results suggest the silica particles are an important layer of protection against erosion. The suspending fluid is vulnerable to AO attack however, and we are testing silicone coatings on a current MISSE-13 mission to test their durability in the LEO environment. Note, the effect on material flexibility from the apparent cross-linking on the surface of the Orthofabric has not been investigated yet. Additionally, the increase in solar absorbance of the treated Orthofabric can have negative ramifications for the heat rejecting properties of the suit and warrants future studies.

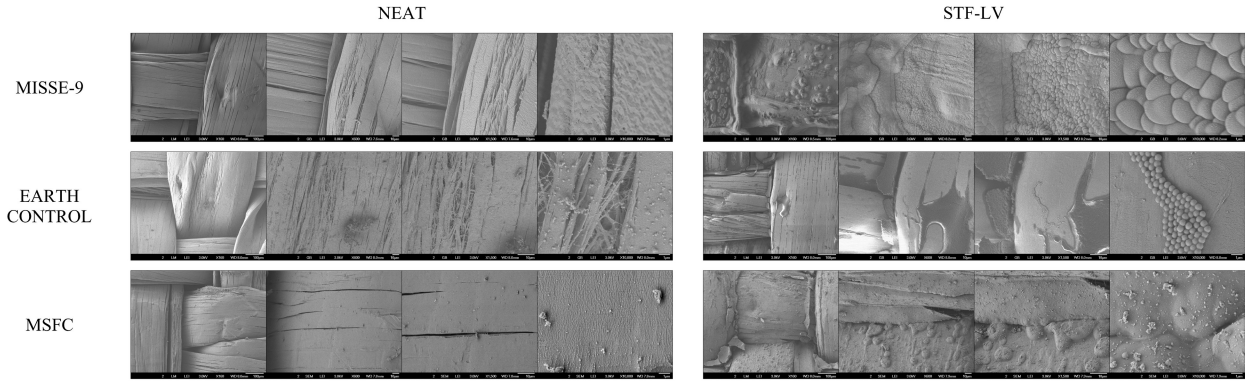

Figure 15. SEM image comparison of the Gore-Tex® side of Orthofabric, non-treated and STF-LV treated.

VII. Conclusion

A variant of the current TMG of the EVA space suit with an advanced nanocomposite modification has been successfully tested in LEO on the MISSE platform, mission MISSE-9. Samples tested comprise a neat layup and an STF-Armor layup, where the Orthofabric and Spectra® layers are treated with a shear thickening colloidal suspension formulated to enhance the puncture resistance of the layup while withstanding the high-vacuum condition of LEO. Space environment simulation studies of HVI ballistic response and AO erosion demonstrate that the LEO-compliant STF-Armor modified materials maintain mechanical performance characteristics with somewhat diminished optical properties compared to the non-treated materials. The mission post-flight testing revealed unanticipated benefits to the puncture resistance after extended LEO exposure, suggesting a synergistic effect from the presence of AO and solar radiation in LEO environment. While ground-based studies of AO exposure did not show any significant changes in absorptivity or emissivity, extended LEO exposure resulted in a discoloration of the STF-treated Orthofabric, which increased absorptivity. This is postulated to be due to the UV exposure of the STF carrier fluid. This knowledge is helpful to guide future formulation development improvements and future MISSE mission tests. Moreover, these flight results contribute to the TRL advancement of TMG space suit materials.

Acknowledgments

M.K. acknowledges financial support from Delaware Space Grant Consortium under grants 80NSSC20M0045 and NNX15AI19H. This work was completed in part under NASA EPSCoR award NNX14AK99A and supported at STF Technologies LLC by NASA STTR contracts NNX16CJ29P and 80NSSC17C0025.

References

[1]B. Peters and H. H. Tang, "Developing NASA's next-generation spacesuit," *Spec. Fabr. Rev.*, 2018.

[2]N. C. Jordan, J. H. Saleh, and D. J. Newman, "The extravehicular mobility unit: A review of environment, requirements, and design changes in the US spacesuit," *Acta Astronaut.*, vol. 59, no. 12, pp. 1135–1145, 2006.

[3]S. Ryan, E. L. Christiansen, B. A. Davis, and E. Ordonez, "Mitigation of EMU Cut Glove Hazard from Micrometeoroid and Orbital Debris Impacts on ISS Handrails," 2009.

[4]M. M. S. Mousavi *et al.*, "Spacesuits and EVA gloves evolution and future trends of extravehicular activity gloves," 2011.

[5]A. Ross, R. Rhodes, and S. McFarland, "NASA Advanced Space Suit Pressure Garment System Status and Development Priorities 2019," 2019.

[6]A. Ross, R. Rhodes, and S. McFarland, "NASA's Advanced Extra-vehicular Activity Space Suit Pressure Garment 2018 Status and Development Plan," 2018.

[7]N. J. Wagner and J. F. Brady, "Shear thickening in colloidal dispersions," *Phys. Today*, vol. 62, no. 10, pp. 27–32, 2009.

[8]C. D. Cwalina and N. J. Wagner, "Material properties of the shear-thickened state in concentrated near hard-sphere colloidal dispersions," *J. Rheol. (N. Y. N. Y).*, vol. 58, no. 4, pp. 949–967, 2014.

[9]M. J. Decker, C. J. Halbach, C. H. Nam, N. J. Wagner, and E. D. Wetzel, "Stab resistance of shear thickening fluid (STF)-treated fabrics," *Compos. Sci. Technol.*, vol. 67, no. 3, pp. 565–578, 2007.

[10]Y. S. Lee, E. D. Wetzel, and N. J. Wagner, "The ballistic impact characteristics of Kevlar ® woven fabrics impregnated with a colloidal shear thickening fluid," *J. Mater. Sci.*, vol. 38, no. 13, pp. 2825–2833, 2003.

[11]R. Dombrowski, N. Wagner, M. Katzarova, and B. Peters, "Development of Advanced Environmental Protection Garments Containing Shear Thickening Fluid Enhanced Textiles (STF-ArmorTM) for Puncture Protection and Dust," 2018.

[12]C. D. Cwalina, R. D. Dombrowski, C. J. McCutcheon, E. L. Christiansen, and N. J. Wagner, "MMOD Puncture Resistance of EVA Suits with Shear Thickening Fluid (STF)--ArmorTM Absorber Layers," *Procedia Eng.*, vol. 103, pp. 97–104, 2015.

[13]M. M. Finckernor, "Comparison of High-Performance Fiber Materials Properties in Simulated and Actual Space Environments," 2017.

[14]A. Finchum, M. Nehls, W. Young, P. Gray, B. Suggs, and N. M. Lowrey, "Capabilities of the Impact Testing Facility at Marshall Space Flight Center," 2011.

[15]E. L. Christiansen, B. G. Cour-Palais, and L. J. Friesen, "Extravehicular activity suit penetration resistance," *Int. J. Impact Eng.*, vol. 23, no. 1, pp. 113–124, 1999.

[16]E. Grossman and I. Gouzman, "Space environment effects on polymers in low earth orbit," *Nucl. Instruments Methods Phys. Res. Sect. B Beam Interact. with Mater. Atoms*, vol. 208, no. 1–4, pp. 48–57, 2003, doi: 10.1016/S0168-583X(03)00640-2.